Tellus (1984), *36A*, 64–75

Available potential energy and extratropical cyclone activity during the FGGE year

By THOMAS L. KOEHLER and KYUNG DUCK MIN[1], *Department of Meteorology, University of Wisconsin, Madison, Wisconsin 53706, U.S.A.*

(Manuscript received January 20; in final form April 26, 1983)

ABSTRACT

Available potential energy quantities derived using twice daily Northern Hemisphere data are compared to extratropical cyclone activity during the First GARP Global Experiment (FGGE) year. The so-called exact (isentropic) available potential energy formulations are employed, both for the entire hemisphere and within limited regions.

Good agreement is indicated between cyclone tracks and hemispheric distributions of the time mean and standard deviations of eddy available potential energy contributions by individual 5° latitude–longitude areas during each season of the FGGE year. The regional available potential energies in climatologically active east coast cyclogenetic regions are shown to exceed values from less active eastern ocean regions during active periods of cyclogenesis. Also, regional available potential energy values from four Northern Hemisphere quadrants suggest that asymmetries in the land–ocean distributions of the hemisphere may be responsible for the diurnal variation in hemispheric available energy values reported in previous work. As indicated by these results, it is important to use limited region calculations when studying atmospheric features that derive their energy on scales smaller than the entire hemisphere.

1. Introduction

Extratropical cyclones not only affect the day-to-day weather in mid-latitudes, but also play a crucial role in the general circulation of the atmosphere, especially in the transport of energy from the tropics to polar regions. Climatological studies by Petterssen (1956), Klein (1957) and Whittaker and Horn (1982) have consistently shown that extratropical cyclogenesis in the Northern Hemisphere occurs in preferred geographical regions, primarily along the east coasts of Asia and North America, and in the lee of prominent mountain ranges.

As first noted by Margules (1903), extratropical cyclones derive much of their kinetic energy from the potential energy available in baroclinic configurations of atmospheric mass fields. Thus, it is not surprising that many of the cyclogenetic regions are also some of the most baroclinic regions. For example, upper level wind climatologies such as Lahey et al. (1960) exhibit wind maxima along the east coastal regions of Asia and North America, consistent with a deep layer of thermal contrast along the coast, and representing a large reservoir of energy available for cyclone development.

Ongoing research at the University of Wisconsin is investigating the role of available potential energy in the formation and development of extratropical cyclones within these cyclogenetically active regions. A previous article by Min and Horn (1982) presented twice daily comparisons of hemispheric available potential energy results computed using both the so-called approximate and exact formulations for the entire FGGE year (December 1978 through November 1979). They concluded that the exact form provides a more realistic picture of the available potential energy patterns through the annual cycle, due to its greater sensitivity to static stability variations. The results

[1] Present affiliation: Department of Earth Sciences, Kyungpook National University, Taegu 635, Korea.

to be presented here continue using the exact form with the same FGGE level IIIa data set employed by Min and Horn (1982). However, the emphasis of this paper is on relating certain aspects of cyclone activity and available potential energy during the FGGE year, rather than comparing exact and approximate form values.

Background on computing available potential energy with both regional and hemispheric reference states is presented in Section 2 of this paper, followed by a brief description of the data set and computational methods in Section 3. Results are arranged in three sections. Section 4 expands the winter season comparisons between the eddy and available potential energy and cyclone frequency presented by Min and Horn (1982) to the remaining FGGE year seasons. Annual time series of daily available potential energy values for regions located over eastern and western portions of the North Atlantic and North Pacific oceans are discussed in Section 5. Finally, diurnal fluctuations in available potential energy values calculated from the FGGE data sets and their possible effect on cyclone activity are discussed in Section 6.

As noted by Min and Horn (1982), dramatic differences appear between the exact and approximate form depictions of available potential energy distributions, especially for grid point contributions to a region's total value. Because some of the exact (isentropic) form results are difficult to interpret by those familiar with the approximate formulations, we have inserted detailed explanations of the exact form depictions at several points in the text to aid the reader's understanding of the results.

2. Background

Lorenz (1955) defined available potential energy (hereafter referred to as APE) as the total potential energy difference between an existing atmospheric mass field and a simpler hypothetical reference atmosphere that could be achieved by an adiabatic redistribution of the existing mass field to a horizontally stratified, statically stable state. Other viable reference states could also be defined, such as those presented by van Mieghem (1956) and Pfeffer et al. (1966). Thus, while the atmosphere over a specified region of the globe has only one total potential energy value, it can have several APE values, one for each plausible reference state. One common example illustrates this point. The APE for a hemisphere or the globe is often separated into zonal and eddy parts. Conceptually, this involves a two-step redistribution of the existing mass field through two reference states. The first redistribution is only in the east–west direction (within individual zonal rings) yielding a zonally symmetric reference state. The total potential energy difference between this state and the original mass redistribution is the eddy APE. To derive the second reference state in this example, this zonally symmetric reference state is uniformly redistributed in the meridional direction over the entire hemisphere (or globe) yielding a horizontally stratified reference state. Subtracting the total potential energy of this final reference state from the original total potential energy produces the total APE (sum of the zonal and eddy components), while the zonal component is determined from the difference between the two reference states. Thus, meaningful results can be obtained from two viable reference states defined from the same initial mass distribution.

Available potential energy has been evaluated for a wide variety of regions. Many general circulation studies have used reference states derived either for the Northern Hemisphere or the entire globe. See for example Oort (1964), Peixoto and Oort (1974), Newell et al. (1974), Oort and Peixoto (1976), and Min and Horn (1982). APE has also been applied by other investigators to study atmospheric features that derive their kinetic energy primarily on scales much smaller than the global scale. For example, Hahn and Horn (1969), Johnson (1970), Gall and Johnson (1971), Bullock and Johnson (1971, 1972), Vincent et al. (1977), Lin and Smith (1979) and Wei (1979) have studied APE and its generation within individual extratropical cyclones. As noted by Johnson (1970), the application of global reference states to these limited regions is inappropriate and reference states derived from the mass redistribution only within the region of study are employed. For regions of intermediate size (between the hemispheric and extratropical cyclone scales) both regional and hemispheric (or global) reference states can provide useful APE information. The APE for a limited region determined from a hemispheric or global reference state represents the contribution by that region to the global or hemispheric APE. For example Smith and Horn (1969) estimated global contributions by North America in this manner for 1 month (March 1962). An APE value determined from a regional redistribution of mass measures the energy available from the regional baroclinity, and thus provides an upper bound for the kinetic energy that could be produced within the region *if* it acted independently from its surroundings. Thus, Johnson (1970) referred to this APE determined from the regional reference state as the baroclinic contribution. Johnson also defined the difference in the total potential energies between the global and regional reference states as the region's barotropic contribution, because it becomes available to the larger region only through boundary processes in an energy exchange between the regional and hemispheric (or global) scales.

In subsequent sections of this paper, both regional and hemispheric reference states are used in defining the APE. A comparison of the baroclinic and barotropic contributions of the cyclogenetically active east coast of Asia is presented in Section 5.

3. Computational methods and data sets

As noted in the previous section, available potential energy (APE) is defined as the difference between the total potential energy of a given atmospheric state (Π) and the total potential energy of some reference state (Π_R)

$$\mathrm{APE} = \Pi - \Pi_R \tag{1}$$

The APE calculations presented in this study were made in the same manner as by Min and Horn (1982), and involve computing Π and Π_R separately, then determining the APE from eq. (1). The total potential energy for a given region (not necessarily the entire hemisphere) can be expressed as,

$$\Pi = \int_s \left\{ \frac{c_p}{g p_{00}^{\kappa}(1+\kappa)} \left[\theta_s p_s^{\kappa+1} - \theta_t p_t^{\kappa+1} + \int_{\theta_s}^{\theta_t} p^{\kappa+1}\, \mathrm{d}\theta \right] \right\} \mathrm{d}S \tag{2}$$

where c_p is the specific heat at constant pressure, g is the gravitational acceleration, κ is the ratio of the gas constant (R_d) to c_p, p is pressure, θ is potential temperature and S is the surface area of the region. The s and t subscripts denote the earth's surface and the upper isentropic boundary respectively. A similar expression is used to determine Π_R, replacing the p and θ values with their reference atmosphere counterparts. The reference atmosphere is determined from the initial mass distribution using an iterative method described by Koehler (1979), a technique similar to that presented by Taylor (1979). In the free atmosphere (where isentropes do not intersect the earth's surface) the reference pressure for a given isentropic surface is defined by the area-averaged pressure on that isentropic surface. The redistribution of mass for lower isentropic levels is done iteratively to properly account for the earth's topography. Once the pressure distribution on isentropic surfaces for both the original and reference atmospheres are defined, the APE value within a given region can be computed.

The FGGE level IIIa data set provides the data used in these APE computations. This data set consists of gridded temperature, height, wind and moisture analyses on mandatory isobaric levels prepared by the National Meteorological Center (NMC) of the U.S. National Weather Service on a twice daily basis from 1 December 1978 to 30 November 1979. (See Bergman, 1979, and McPherson et al., 1979, for details of the data assimilation system that produced the FGGE level IIIa data sets.) These isobaric analyses were interpolated vertically to 16 isentropic levels spaced at 10 K starting as low as 220 K and extending to at least 370 K by Townsend (1980). This interpolation produced horizontal p on θ distributions at $2\frac{1}{2}°$ latitude–longitude intersections over the entire globe. A Northern Hemisphere subset of these gridded isentropic analyses for only those grid points centered in 5° latitude–longitude boxes were used both in this study and by Min and Horn (1982).

The FGGE year cyclone tracks and cyclogenesis frequency values, presented in later sections were compiled by Whittaker (1982, personal communication) from standard NMC products using a method presented in Whittaker and Horn (1981, 1982). Over the oceans and North America, tracks produced routinely at NMC and presented in the *Mariners Weather Log* and the *Climatological Data, National Summary* were employed. Cyclones over Eurasia were tracked from the Northern Hemisphere Surface Charts, 6 hourly NMC surface analyses available on microfilm.

4. Comparisons of eddy APE distributions to seasonal cyclone tracks

As mentioned in Section 2, the eddy APE represents the energy that might be realized from an east-west mass redistribution of a zonally asymmetric original state to a zonally symmetric reference state. The circulation around extratropical cyclones in the Northern Hemisphere draws warmer air northward ahead of the cyclone and colder air southward behind the low, accentuating zonal asymmetries in the mass field. Thus, a relationship between eddy APE and extratropical cyclone activity might be expected. In this section, seasonal cyclone tracks from the FGGE year are compared to seasonal means and standard deviations of twice daily eddy APE quantities. The winter (DJF) results were originally presented in Min and Horn (1982).

Since extratropical cyclones occur in preferred regions, it is important to present comparisons between cyclone activity and eddy APE in a

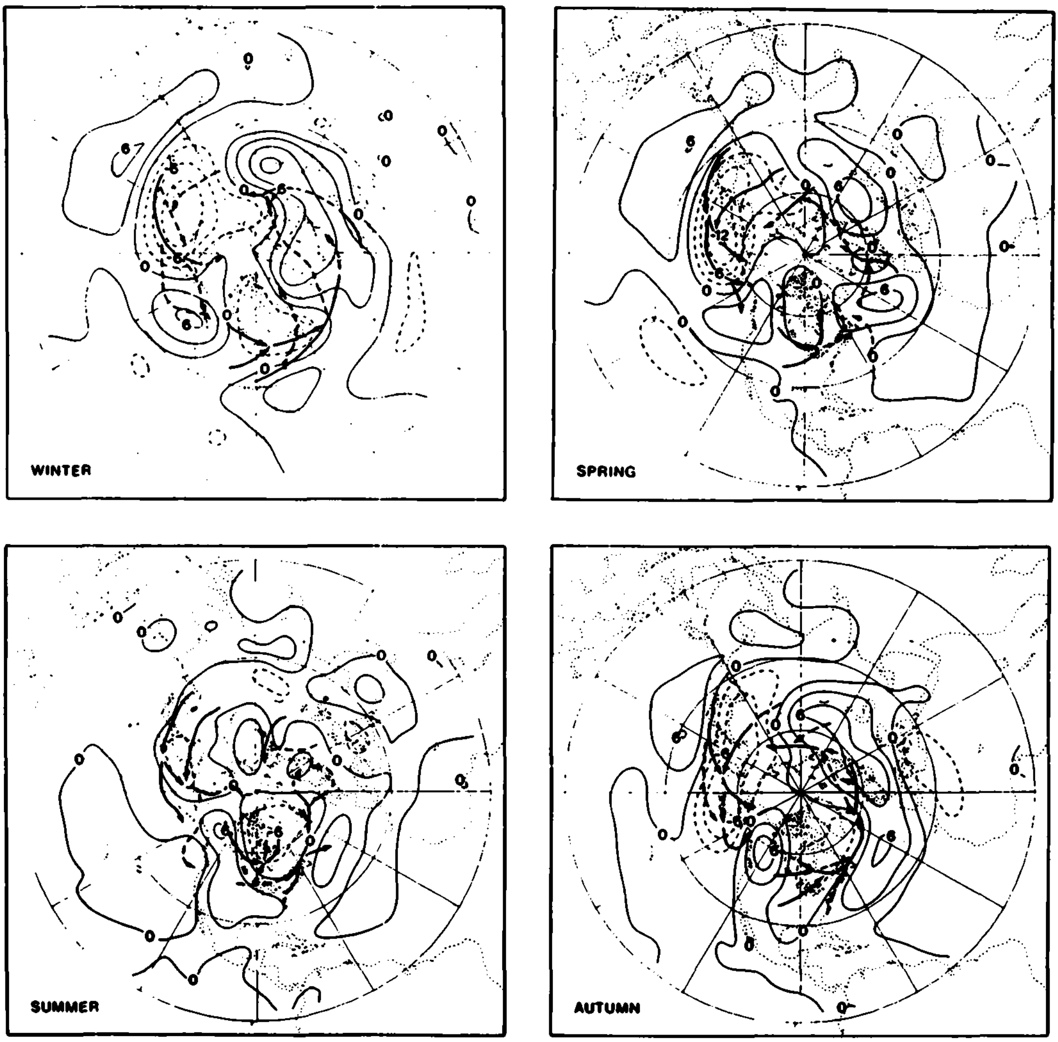

Fig. 1. Geographical distributions of the mean contributions to the total hemispheric eddy APE (10^3 J kg^{-1}) by 5° latitude–longitude areas for each season of the FGGE year, and the corresponding extratropical cyclone tracks. Primary tracks are solid, and secondary tracks dashed.

geographical format. While eddy APE is a hemispheric quantity, it can be represented as a sum of contributions from smaller, finite regions. In this study, contributions to the eddy APE for each 5° latitude–longitude region of the Northern Hemisphere were computed on a twice daily basis throughout the FGGE year. These contributions were normalized by the mass within the region to account for varying region size, and to minimize the response in the energy contribution attributable to changes in surface pressure. Means and standard deviations of these specific (per unit mass) eddy APE contributions were computed for each season, and horizontal analyses of these statistics are presented in Figs. 1 and 2, with cyclone tracks from the FGGE year superimposed. Normally, cyclone tracks are compiled on a monthly basis. Only a limited number of cyclones are available from a 1-year sample, making it necessary to combine 3 months of data (a season) to produce meaningful composite storm tracks. In the first two figures, the most preferred (primary) tracks are indicated with thick solid lines, while less frequent (secondary) tracks are dashed.

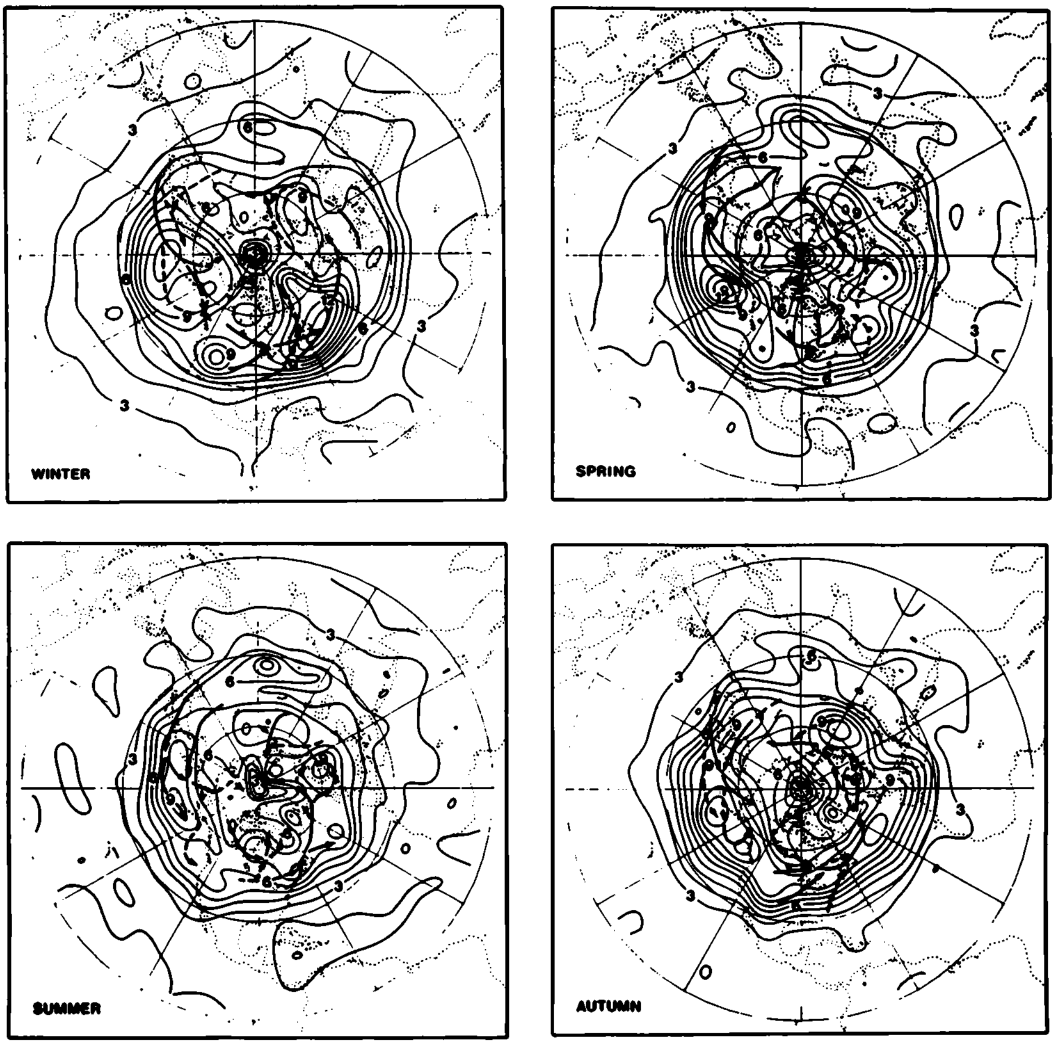

Fig. 2. Same format as Fig. 1, except seasonal standard deviations of the twice daily APE contributions (10^3 J kg^{-1}) are presented instead of the seasonal means.

The seasonal means of the eddy APE contributions shown in Fig. 1 have both positive and negative values, as opposed to the approximate form results shown in Fig. 5a in Min and Horn (1982) which has smaller but positive contributions over the entire hemisphere. It is worthwhile at this point in the discussion to clarify that both positive and negative contributions are not only possible, but expected in the exact form.

Eddy available potential energy is in essence a relative quantity, being expressed as the total potential energy difference between an actual atmospheric state, and a reference atmosphere derived from the actual state by a redistribution of the mass field within individual zonal rings. Consider a hypothetical east–west isentropic cross section through one of these zonal rings which, for the sake of simplifying the discussion, is over uniform terrain. Isentropes in the actual atmosphere would slope in baroclinic regions from high pressure in warm regions to low pressure in cold regions. In contrast, isentropes in the reference atmosphere would be horizontal, appearing at the average pressure on the original isentropic surface. The contribution by each 5° region to the reference total potential energy would be constant for each region in the latitudinal ring, but the actual total potential energy contributions would vary between maximum values primarily in warmer regions and minimum values primarily in colder regions. For entropy to be conserved in the mass redistribution, the regional reference total potential energy will fall somewhere between the maximum and minimum values in the original state, as some air parcels rise and cool adiabatically, while others sink and warm. Since the APE is the difference between these total potential energies, regions with maximum total potential energy values in the original state will have positive APE contributions, while those near the minimum will have negative contributions. Only the sum of the contributions for the zonal ring is necessarily positive.

Essentially, the APE contributions provide a measure of the relative thermal content of a given column of atmosphere. Baroclinic situations exhibit greater horizontal variation in these contributions and also yield greater total APE values than more barotropic configurations. The total APE thus provides an integrated measure of the baroclinity within the chosen domain.

The seasonal mean contributions shown in Fig. 1 highlight the more stationary long wave features of the hemispheric circulation. First, consider the winter situation, with significant negative values associated with colder atmospheric columns centered over the Kamchatka Peninsula and Hudson Bay, and the positive centers of warmer atmospheric columns off the west coast of North America, from Scandinavia into central Asia, and in the Pacific south of Japan. Gradients in these contributions are found in baroclinic regions. Note, for example, the strong average baroclinity south of Japan, where one of the primary winter storm tracks originates. Gradients in the mean APE contributions are also strong in spring and autumn, with a weaker pattern during the less active summer months. The northwest Pacific maintains the dominant negative contributions for three of the four seasons, with the largest negative values over Hudson Bay only during the summer.

The variability of eddy APE contributions associated with the movement of extratropical cyclones is lost in the seasonal averaging. However, the standard deviations shown in Fig. 2 do measure the temporal variability of the APE contributions within the 5° regions. These standard deviations are affected not only by the propagating short waves associated with extratropical cyclones, but also by changes on other time scales, such as diurnal fluctuations, the development and movement of long-wave patterns over the period of a week or more, and long-period trends through the entire season. Fortunately, the long-period trends mainly influence the zonal APE, and the amplitude of the diurnal changes within 5° areas is small compared to those from daily and weekly changes. Thus, synoptically active short waves and the more slowly moving long waves provide most of the signal in these standard deviations. Computing the statistics over periods of a few weeks or a month instead of a season might reduce the influence of the longer waves, but would preclude comparisons against composite storm tracks.

The results in Fig. 2 indicate a reasonable, though not perfect correspondence between the cyclone tracks and maxima in the APE contribution standard deviations. For example, storm tracks in mid-ocean fit the standard deviation patterns well for all seasons, but the tracks originate in regions with smaller standard deviations along the east coast of Asia and North America. In a physical sense, this might be expected. Cyclogenesis along the east coasts feeds off the baroclinity inherent to the region, as indicated by the tracks originating in regions of strong mean contribution gradients (see Fig. 1). Strong asymmetries in the zonal thermal pattern (which contribute to greater standard deviations) appear only after the circulation has appreciably developed around the storm center, primarily during the mature stage. Thus the maximum standard deviations should appear downstream from the cyclogenetic region.

Another factor to consider is that the strength of cyclones is usually not used in compiling cyclone tracks. Thus a primary storm track composed of weaker lows with little baroclinic development would probably have a weaker signature in the standard deviation pattern than a secondary track composed of deeper lows.

In any event, these exact form eddy APE contributions do exhibit a reasonable relationship to the cyclone tracks for the entire FGGE year. As indicated in Min and Horn (1982), for the winter season, this relationship could not be discerned from approximate form results.

5. Regional APE estimates in cyclogenetic regions

The comparisons just shown between eddy APE and cyclone tracks are useful in identifying their hemispheric interrelationships. Recall that eddy APE is a hemispheric property with contributions from a particular region dependent on mass configurations on the other side of the hemisphere. As noted earlier, energy conversions associated with the formation and development of extra-tropical cyclones are more regional in nature, involving both the north–south and east–west distributions of potential energy. In this section, FGGE year time series of regional APE estimates for the active cyclogenetic east coast regions of Asia and North America are compared to regional estimates from less active regions over the eastern oceans. These four regions are outlined in Fig. 3.

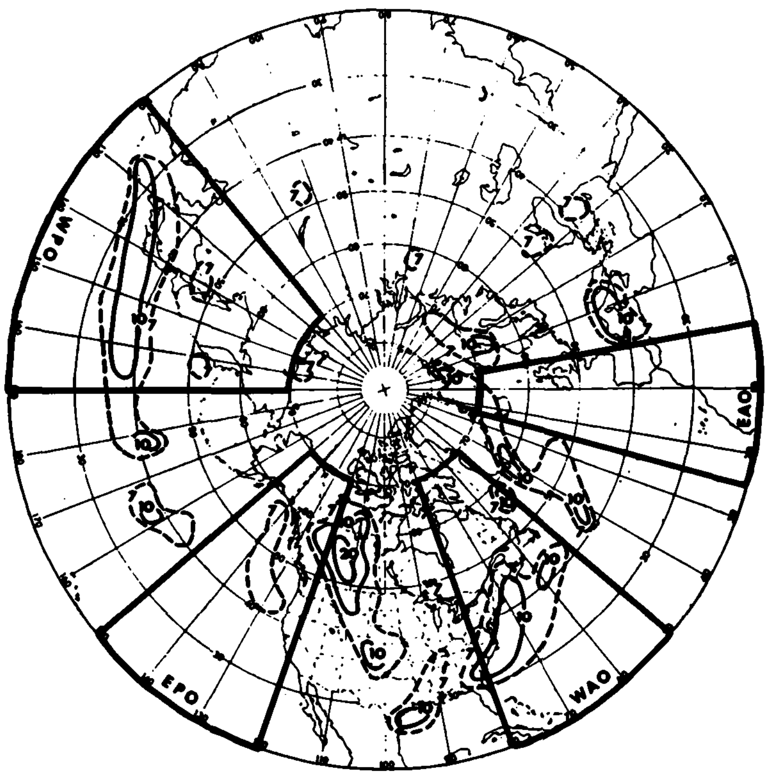

Fig. 3. January cyclogenesis frequencies from Whittaker and Horn (1982) for the 20-year sample 1958–1977 and regions chosen for closer examination. The western Pacific (WPO) and western Atlantic (WAO) regions are more active cyclogenetic regions than their eastern ocean counterparts (EPO and EAO, respectively).

The selection of these regions was based on a climatology of January cyclogenesis frequencies compiled by Whittaker and Horn (1982) for the 20-year period 1958–1977. As shown in Fig. 3, the western Pacific and western Atlantic regions (WPO and WAO, respectively) are climatologically active cyclogenetic regions, while the eastern Atlantic and eastern Pacific regions (EAO and EPO) are less active. Greater regional APE values might be expected in the western ocean regions (the east coasts) than over the eastern oceans during the active winter and spring cyclogenetic seasons.

This is generally the case for the FGGE year, as Fig. 4 illustrates. More separation is evident between the Pacific regions than between the Atlantic regions. In fact, EAO values exceed the WAO values during much of the spring. Climatologically, spring is an active season for cyclogenesis off the east coast of the United States. This was not the case during the FGGE year however, as indicated by the absence of any cyclone track, either primary or secondary, in that region in the spring panels of Figs. 1 and 2. Furthermore, the frequency of cyclogenesis in all four regions during the FGGE year fell substantially below averages from the 20-year Whittaker and Horn (1982) sample (see Table 1), a result consistent with the decrease in North American cyclogenesis reported by Zishka and Smith (1980) and Whittaker and Horn (1981). Note in Fig. 1, the gradients in the mean spring eddy APE contributions were also weak along the east coast of North America during the FGGE year. This is indicative of weak baroclinity in that region during spring 1979, and therefore less regional APE to fuel cyclogenesis.

Table 1. *Yearly cyclogenesis events (per 5° longitudinal extent) for four ocean regions during the FGGE year and the average from the Whittaker and Horn (1982) 20-year sample (1958–1977)*

Region	Mean 1958–1977	FGGE year
WPO	19.3	15.3
EPO	15.7	10.7
WAO	20.4	15.5
EAO	13.1	11.0

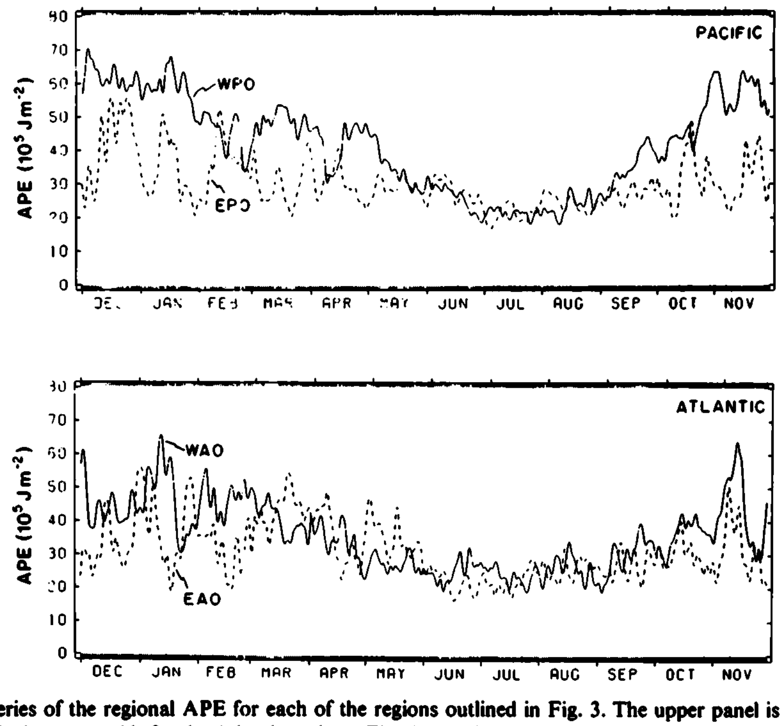

Fig. 4. Time series of the regional APE for each of the regions outlined in Fig. 3. The upper panel is for the Pacific regions, while the lower panel is for the Atlantic regions. The time series were filtered to remove diurnal variations.

Another interesting feature in Fig. 4 is the relatively large regional APE maintained in the WPO region during December and January and reappearing in late October and November. The very cold air on the eastern edge of the Siberian high is situated in the northwest corner of the WPO area. The cold northerly winds circulating around this anticyclone transport colder air off the continent over the western Pacific, producing much of the baroclinity in this region. Thus, a decrease in the WPO APE during late January and February indicates a weakening of the region's baroclinity probably due to a weaker Siberian anticyclone.

The WPO region can also be used to illustrate the importance of using regional reference states in cyclogenesis studies. Some of the coldest air in the Northern Hemisphere is found in this region during three-quarters of the year, as indicated by the large negative eddy APE contributions at 50° N in Fig. 1. These eddy values are relative to zonal mean reference states. Since the zonal reference state at 50°N is much colder than that from a tropical latitude, (say 10°N), the hemispheric total APE contributions would be even more negative. This is illustrated in Table 2, where monthly mean contributions by the WPO region to the hemispheric total APE are presented. This negative contribution is largest in magnitude during the winter months, with the magnitude of this negative value decreasing as the north–south temperature gradients weaken during the spring and summer. The monthly mean regional APE values (the baroclinic contribution) are also presented in this table. As expected the maximum winter baroclinity is reflected in larger positive regional APE's. Thus, the hemispheric contribution of this region exhibits minimum winter values, and maximum summer values, while the reverse is true for the regional APE. Since cyclogenesis responds primarily to changes in regional APE, applying results from hemispheric references states in cyclone studies could be misleading. The barotropic contributions also shown in Table 2 emphasize how cold the regional reference states are compared to the hemispheric reference state in that region (used to determine the hemispheric contribution).

Table 2. *The monthly mean contributions of the WPO region to the hemispheric total APE (10^5 J m^{-2}) subdivided into its baroclinic and barotropic components*

Month	Hemispheric contribution	Baroclinic component	Barotropic component
December	−752.6	62.0	−814.6
January	−883.4	58.8	−942.2
February	−756.7	45.1	−801.8
March	−843.0	48.3	−891.3
April	−576.9	42.4	−619.3
May	−405.1	34.4	−439.5
June	−274.1	25.8	−299.8
July	−233.0	21·4	−254.4
August	−207.2	23.3	−230.5
September	−270.2	34.0	−304.2
October	−428.9	45.3	−474.2
November	−537.9	57.4	−595.3

6. Diurnal variations in the APE results

The twice daily hemispheric APE results presented in Fig. 1 of Min and Horn (1982) exhibit a diurnal oscillation, expecially during the summer months. Diurnal variations in the thermal structure of the atmosphere reflected in this APE response result from complicated interactions of several factors, such as surface heating and cooling, variations in cloudiness and diurnal wind fluctuations. The primary forcing for many of these factors is the diurnal cycle in heating and cooling the earth's surface by radiative processes. While a diurnal APE response might be expected over a limited region, obtaining this response in a quantity integrated over the entire hemisphere is moderately surprising. If, for example, the surface features of the hemisphere were homogeneous (either all land or all ocean), little or no diurnal fluctuation would be evident in hemispheric totals, because the response to heating or cooling would also be symmetric, following the sun in its westward propagation around the earth. However, the land–ocean distribution in the Northern Hemisphere is definitely asymmetric, which contributes to a diurnal response in the hemisphere APE totals.

To isolate these effects, the Northern Hemisphere was subdivided into four quadrants (Q1: 10° W to 80° E, Q2: 80 °E to 170° E, Q3: 170° E to 100° W, and Q4: 100° W to 10° W), and regional APE values were determined for each quadrant. While all four quadrants have a mixture of land and ocean surfaces, Q1 is predominantly land, and Q3 on the opposite side of the hemisphere is predominantly ocean. Monthly mean regional APE values from these quadrants for both 0000 GMT (solid) and 1200 GMT (dashed) are presented in Fig. 5. The APE values for all four regions exhibit an annual cycle associated with the weakening and strengthening of the north–south temperature gradient through the course of the year. The maximum diurnal changes (evident from differences between 0000 GMT and 1200 GMT) are larger in summer, the season of minimum APE values. Summer is also the period of high solar zenith angles in the Northern Hemisphere. Region Q1 exhibits the greatest diurnal change, with larger APE values at 1200 GMT than at 0000 GMT. Two factors contribute to the large diurnal signal in region Q1: the timing of the upper air observations, and land–ocean configurations. The mid-afternoon peak in surface temperatures occurs at roughly 1200 GMT in region Q1, and 0000 GMT corresponds to a period of minimum temperatures. Thus, the time sampling would produce a larger response in Q1 than in the adjacent quadrants, Q2 and Q4. Using this reasoning, region Q3 should exhibit similar changes, only with times at the minimum and maximum reversed. While the reversal is evident in Q3, its diurnal differences are much smaller than those in Q1, because Q3 is an ocean region while Q1 is primarily a land region. The amplitudes of surface temperature changes are particularly large in the subtropical deserts of North Africa and the Middle East, compared to the subtropical Pacific, accounting for the greater diurnal variation in regional APE values in region Q1 than in Q3. This imbalance between the diurnal responses of these two regions accounts for the net diurnal variation in the hemispheric totals.

The major east coast cyclogenetic regions are found in quadrants Q2 and Q4. These regions also exhibit diurnal APE tendencies, but not of the magnitude of region Q1. If available, analyses at 0600 GMT and 1800 GMT would probably show greater diurnal variation over the cyclogenetic regions (Q2 and Q4) than those available at 0000 GMT and 1200 GMT. To carry this reasoning one step further, a diurnal response in the APE for cyclogenetic regions might suggest a preferred time for the onset of cyclogenesis. This possibility is yet to be investigated.

7. Concluding remarks

Available potential energy can be applied as a diagnostic measure in evaluating not only the energetics of hemispheric or global circulations, but also in studying atmospheric features that derive

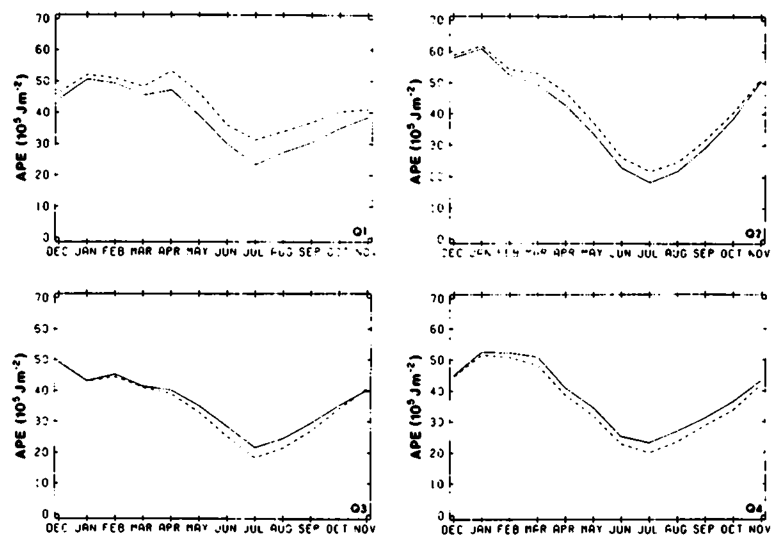

Fig. 5. Monthly mean regional APE values (10^5 J m^{-2}) from the daily 0000 GMT (solid) and 1200 GMT (dashed) APE values for the four hemispheric quadrants: Q1: 10° W–80° E; Q2: 80° E–170° E; Q3: 170° E–100° W; and Q4: 100° W–10° W.

their energy on smaller scales. This article has concentrated on possible relationships between APE and extratropical cyclone activity during the FGGE year. The first set of comparisons illustrated how the geographical distribution of contributions to the hemispheric eddy APE could be related to cyclone activity throughout the entire year. Also, regional APE in cyclogenetic regions was shown to exceed the APE in less active regions during most of the year. Finally, regional APE estimates on a twice daily basis for four Northern Hemisphere quadrants demonstrated that asymmetries in the hemispheric land–ocean distributions are primarily responsible for the diurnal signal in the hemispheric APE observed by Min and Horn (1982).

The exact APE formulation in isentropic coordinates was employed in all the calculations presented here. As noted by Min and Horn (1982), the exact form can produce results that are strikingly different from those from the more familiar approximate formulations. Relationships between APE values and other atmospheric features (such as cyclones) are more clearly depicted in the exact form.

The results presented both in this paper and in Min and Horn (1982) represent only the initial findings from ongoing research into interrelationships between extratropical cyclone activity and atmospheric energetics, especially APE. Further work involves including kinetic energy into these evaluations, and examining in finer detail the interactions between cyclone activity and changes in regional APE on monthly to weekly time scales.

8. Acknowledgements

The authors deeply appreciate Linda Whittaker's contribution to this study, including the compilation of the FGGE year cyclone data and her help with the manuscript and figures. Thanks are also due to Dr. Ron Townsend and Tom Whittaker for providing the isentropic data sets. Dr. Lyle Horn provided valuable assistance and support throughout the study. Finally, we wish to thank Debbie Schiess for typing the final manuscript. This research was supported by NSF Grant ATM 7918761.

REFERENCES

Bergman, K. H. 1979. A multivariate optimum interpolation analysis system of temperature and wind fields. *Mon. Wea. Rev. 107*, 1423–1444.

Bullock B. R. and Johnson, D. R. 1971. The generation of available potential energy by latent heat release in a mid-latitude cyclone. *Mon. Wea. Rev. 99*, 1–14.

Bullock, B. R. and Johnson, D. R. 1972. The generation of available potential energy by sensible heating in Southern Ocean cyclones. *Q. J. R. Meteorol. Soc. 98*, 495–518.

Climatological Data, National Summary, 1978–1979. NOAA/EDIS, U.S. Dept. of Commerce.

Gall, R. L. and Johnson, D. R. 1971. The generation of available potential energy by sensible heating: a case study. *Tellus 23*, 466–482.

Hahn, D. G. and Horn, L. H. 1969. The generation of available potential energy in a mid-latitude cyclone. Studies of large scale atmospheric energetics. Final report ESSA grant WBG-52, University of Wisconsin, 1–56.

Johnson, D. R. 1970. The available potential energy of storms. *J. Atmos. Sci. 27*, 727–741.

Klein, W. H. 1957. Principal tracks and mean frequencies of cyclones and anti-cyclones in the Northern Hemisphere. Res. Pap. No. 40, U.S. Weather Bureau, U.S. Government Printing Office, Washington, D.C., 60 pp.

Koehler, T. L. 1979. A case study of height and temperature analyses derived from Nimbus-6 satellite soundings on a fine mesh grid. Ph.D. thesis, Department of Meteorology, University of Wisconsin-Madison, 162–182.

Lahey, J. F., Bryson, R. A., Corzine, H. A. and Hutchins, C. W. 1960. *Atlas of 300 mb Wind Characteristics for the Northern Hemisphere*. The University of Wisconsin Press, 125 pp.

Lin, S. C. and Smith, P. J. 1979. Diabatic heating and generation of available potential energy in a tornado-producing extratropical cyclone. *Mon. Wea. Rev. 107*, 1169–1183.

Lorenz, E. N. 1955. Available potential energy and the maintenance of the general circulation. *Tellus 7*, 157–167.

Margules, M. 1903. Über die Energie der Stürme, translated by Abbe (1910). *Smithsonian Ins. Misc. Coll. 51*, 553–595.

Mariners Weather Log, 1979–1980. NOAA/EDIS, U.S. Dept. of Commerce.

McPherson, R. D., Bergman, K. H., Kistler, R. E., Rasck, G. E. and Gordon, D. S. 1979. The NMC operational global data assimilation system. *Mon. Wea. Rev. 107*, 1445–1461.

Min, K. D. and Horn, L. H. 1982. Available potential energy in the Northern Hemisphere during the FGGE year. *Tellus 34*, 526–539.

Newell, R. E., Kidson, J. W., Vincent, D. G. and Boer, G. J. 1974. *The General Circulation of the Tropical Atmosphere and Interaction with Extratropical Latitudes*, 2. The MIT Press, 371 pp.

Oort, A. H. 1964. On estimates of the atmospheric energy cycle. *Mon. Wea. Rev. 92*, 483–493.

Oort, A. H. and Peixoto, J. P. 1976. On the variability of the atmospheric energy cycle within a 5-year period. *J. Geophys. Res. 81*, 3643–3659.

Peixoto, J. P. and Oort, A. H. 1974. The annual distribution of atmospheric energy on a planetary scale. *J. Geophys. Res. 79*, 2149–2159.

Petterssen, S. 1956. *Weather Analysis and Forecasting*, Vol. 1, 2nd ed. McGraw/hill, 266–276.

Pfeffer, R. L., Mardon, D., Sterbenz, P. and Fowlis, W. 1966. A new concept of available potential energy. Report No. 66–1, Florida State University, Department of Meteorology.

Smith, P. J. and Horn, L. H. 1969. A computational study of energetics of a limited region of the atmosphere. *Tellus 21*, 193–201.

Taylor, K. 1979. Formulas for calculating available potential energy over uneven topography. *Tellus 31*, 236–245.

Townsend, R. D. 1980. A diagnostic study of the zonally-averaged global circulation in isentropic coordinates. Ph.D. thesis, Department of Meteorology, University of Wisconsin-Madison, 221 pp.

van Mieghem, J. 1956. The energy available in the atmosphere for conversion into kinetic energy. *Beitr. Phys. Atmos. 29*, 129–142.

Vincent, D. G., Pant, G. B. and Edmon, Jr., H. J. 1977. Generation of available potential energy of an extratropical cyclone system. *Mon. Wea. Rev. 105*, 1252–1265.

Wei, M-Y. 1979. The energy budgets of a developing cyclone over the East China Sea during the 1975 Air Mass Transformation Experiment. The University of Oklahoma, Contribution No. 79–1, 136 pp.

Whittaker, L. M. and Horn, L. H. 1981. Geographical and seasonal distribution of North American cyclogenesis, 1958–1977. *Mon. Wea. Rev. 109*, 2312–2322.

Whittaker, L. M. and Horn, L. H. 1982. *Atlas of Northern Hemisphere Extratropical Cyclone Activity, 1958–1977*. Department of Meteorology, University of Wisconsin-Madison, 65 pp.

Zishka, K. M. and Smith, P. J. 1980. The climatology of cyclones and anticyclones over North America and surrounding ocean environs for January and July, 1950–77. *Mon. Wea. Rev. 108*, 387–401.